Accepted Manuscript

Synthesis, COX-1/2 inhibition activities and molecular docking study of isothiazolopyridine derivatives

Piotr Świątek, Malgorzata Strzelecka, Rafal Urniaż, Katarzyna Gębczak, Tomasz Gębarowski, Kazimierz Gąsiorowski, Wieslaw Malinka

PII: S0968-0896(16)31092-6
DOI: http://dx.doi.org/10.1016/j.bmc.2016.10.036
Reference: BMC 13363

To appear in: *Bioorganic & Medicinal Chemistry*

Received Date: 29 July 2016
Revised Date: 25 October 2016
Accepted Date: 29 October 2016

Please cite this article as: Świątek, P., Strzelecka, M., Urniaż, R., Gębczak, K., Gębarowski, T., Gąsiorowski, K., Malinka, W., Synthesis, COX-1/2 inhibition activities and molecular docking study of isothiazolopyridine derivatives, *Bioorganic & Medicinal Chemistry* (2016), doi: http://dx.doi.org/10.1016/j.bmc.2016.10.036

SYNTHESIS, COX-1/2 INHIBITION ACTIVITIES AND MOLECULAR DOCKING STUDY OF ISOTHIAZOLOPYRIDINE DERIVATIVES

Piotr Świątek [a] *, Małgorzata Strzelecka [a], Rafał Urniaż [b], Katarzyna Gębczak [c], Tomasz Gębarowski [c], Kazimierz Gąsiorowski [c], Wiesław Malinka [a]

[a] Department of Chemistry of Drugs, Wrocław Medical University, Borowska 211, 50-556 Wrocław, Poland

[b] Department of Medicine, Institute for Medical Research, University of Cambridge, Cambridge Biomedical Campus, Addenbrooke's Hospital, Hills Rd, CB2 0SP, Cambridge, UK

[c] Department of Basic Medical Science, Wrocław Medical University Borowska 211, 50-556 Wrocław, Poland

ABSTRACT

One of the main challenges for nowadays medicine is drugs selectivity. In COX-1 and COX-2, the active sites are composed of the same group of amino acids with the exception of the only one residue in position 523, in COX-1 is an isoleucine, while in COX-2 is a valine. Here, we presented a series of isothiazolopyridine/benzisothiazole derivatives substituted differently into an isothiazole ring, which were synthesized and investigated for their potencies to inhibit COX-1 and COX-2 enzymes by colorimetric inhibitor screening assay. All the tested compounds inhibited the activity of COX-1, the effect on COX-2 activity was differential. The mode of binding was characterized by a molecular docking study. Comparing biological activity of the investigated compounds, it was observed that compounds sharing the most similar position to flurbiprofen and meloxicam, representing the two main enzyme subdomains, achieved higher biological activity than others. It is directly related to the fit to the enzyme's active site, which prevents too early dissociation of the compounds.

1. INTRODUCTION

Cyclooxygenase (COX) converts arachidonic acid to prostanoids, which include prostaglandins (PGs), prostacyclin, and thromboxane.[1] Prostanoids are important mediators that regulate diverse functions in the cardiovascular, gastrointestinal, urogenital, and nervous

systems, as well as playing crucial roles in immunity and inflammation.[1] There are several cyclooxygenase isoforms: COX-1, a constitutive form expressed in almost all tissues; COX-2, which is predominantly induced and constitutively expressed in a number of tissues (renal medulla, prostate, brain, and endothelium);[1] and COX-3, a COX-1-derived protein, abundantly found in the cerebral cortex and heart.[2] COX-1 is a constitutive, housekeeping enzyme that is ubiquitously expressed and is responsible for prostanoid production in most tissues.[1] In contrast, COX-2 is an inducible enzyme, expressed at sites of inflammation, infection, and cancer, that generates prostanoids important for driving disease pathogenesis.[1,3] However, COX-2 is also constitutively expressed in kidney, gastrointestinal tract, brain, and thymus, without any signs of inflammation.[4] Constitutive COX-2 expression plays a major role in homeostatic function, in development and maintenance of physiological function of those organs.[1]

COX-1 and COX-2 are the therapeutic targets for anti-inflammatory drugs, including ibuprofen, naproxen, diclofenac and piroxicam, as well as newer COX-2 selective inhibitors (coxibs); collectively these drugs are known as nonsteroidal anti-inflammatory drugs (NSAIDs). NSAIDs are among the most commonly taken as the first-line anti-inflammatory therapy.

It is well known that benzothiazole/benzisothiazole, benzoxazole and pyridoisothiazole derivatives possess interesting anti-inflammatory and analgesic activity.[5-12] Compound **A**, for example, shown in Figure 1 exhibited higher antinociceptive activity than aspirin and moderate anti-inflammatory activity in comparison with indomethacin.[7] Moreover, the benzothiazole derivatives **B** were reported to interact with COX-2 enzyme more efficiently than rofecoxib, with anti-inflammatory activity as well.[8] Additionally, compound **C** revealed a better inhibitory profile of induction of edema in the carrageenan-induced paw edema than indomethacin.[9] Furthermore, 4-arylpiperazine derivatives of pyridoisothiazole showed high antinociceptive activity in the writing test, in particular, compounds **22**, **23**, **24** and **25**, which were able to reduce the number of abdominal constrictions by more than 50% at the doses of 1.8-7.8 mg/kg.[11,12]

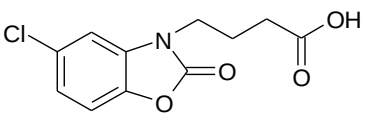

A

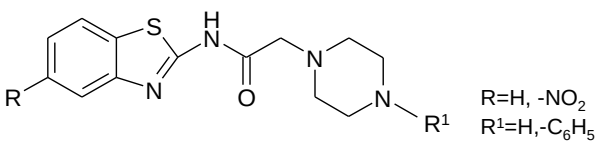

B

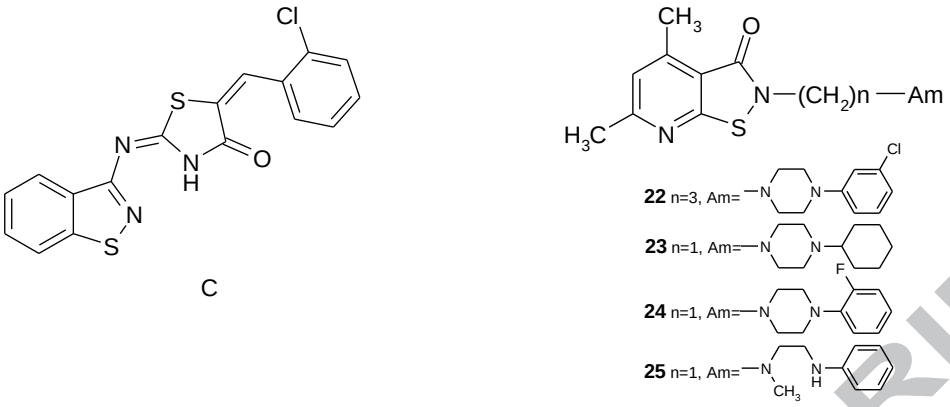

Figure 1. Structures of reference compounds

Considering the above, we designed a group of amide and acid derivatives of isothiazolo[4,5-*b*]pyridine, which can be considered as 7-aza analogues of the benzisothiazole system. The presence of a strong basic and electron-deficient pyridine ring in the isothiazolopyridine moiety makes these systems different from the better known benzoxazole and benzothiazole rings. This study was focused on exploration of the central alkanyl chain length and branching. In order to verify the pharmacological significance of the size and aromaticity of the isothiazolo[4,5-*b*]pyridine moiety, a benzisothiazole derivative was synthesized.

The compounds were investigated for their potencies to inhibit COX-1 and COX-2 enzymes by colorimetric inhibitor screening assay, and the mode of binding was characterized by a molecular docking study

2. RESULTS AND DISCUSSION

2.1 CHEMISTRY

All the new compounds were prepared according to the synthetic pathways outlined in Scheme 1. 4,6-Dimethylisothiazolo[5,4-*b*]pyridin-3(2*H*)-one **1**[13] or commercially available 1,2-benzisothiazol-3(2*H*)-one **2** were used as a starting materials. Compounds **21**-**25** were obtained earlier.[11,12,14]

Preparation of the propanamide derivatives (**8-11**) involves Michael-type addition of isothiazolopyridine **1** or benzisothiazole **2** to corresponding acrylamide derivatives (**3a-c**). Compounds **3a-c** were synthesized by N-acylation of corresponding secondary amines (N-arylpiperazines or 6,7-dimethoxy-1,2,3,4-tetrahydroisoquinoline) with 3-bromopropionyl chloride to give a mixture of acrylamides **3a-c** and 3-bromopropanamides **26a-c** which were separated by CC (Scheme 2). 3-Bromopropanamide derivatives proved to be unstable under

the reaction conditions, and heating in acetonitrile in the presence of potassium carbonate led to dehydrohalogenation of bromopropanamides to give α,β-unsaturated amides (**3a-c**).

Synthesis of the acetamide derivatives (**12** and **13**) was started by obtaining 1-chloroacetyl-4-(3-chlorophenyl)piperazine (**4**) and 1-(2-bromobutanoyl)-4-phenylpiperazine (**5**), respectively. N-acylation of N-arylpiperazines with corresponding chloroacetyl chloride or 2-bromobutyryl bromide led to **4** or **5** without any by-product. Then, the treatment of isothiazolopyridine **1** with intermediates **4** or **5** in acetonitrile in the presence of potassium carbonate provided target compounds (**12** and **13**).

Hydrolysis of esters **7a**, **6b** and **7b** in the presence of an acid catalyst afforded the corresponding acid derivatives (**14**, **15** and **16**)**.** The experimental details for the preparation of esters **6b** and **7b** were recently described.[15] Ethyl 2-[(4,6-dimethylisothiazolo[5,4-b]pyridin-3-yl)oxy]propanoate (**7a**) was obtained by reaction of isothiazolopyridine **1** with ethyl 2-bromopropanoate to give a mixture of 2-N- (**6a**) and 3-O-alkylated (**7a**) isomers which were separated by CC. The yield of 2-N-alkylated isomer was low, and this compound is not described here.

The isomeric butanamides **17-20** were prepared after treatment of 2-N- or 3-O-butanoic acid of isothiazolopyridine (**15** or **16**) with ethyl chloroformate in the presence of trimethylamine, and in the subsequent step, the appropriate amine derivative [1-(3-chlorophenyl)piperazine or 1-phenylpiperazine] was added.

Final compounds were characterized by a sharp melting point (m.p.), correct elemental (C, H, N) analyses, IR and ^{1}H NMR spectra. The structures of the isomeric isothiazolopyridines (**14-20**) were assigned on the basis of ^{1}H NMR. In the 2-N-substituted isomer **15**, **17** and **19** the signal of the methylene protons adjacent to the 2-N-nitrogen of the isothiazolopyridine **1** was recorded within 3.81-3.97 ppm. The 3-O-substitution (**14**, **16**, **18**, **20**) produced downfield shift of these protons in the range 4.46-4.59 ppm. The above spectral data agree with those previously reported for related isomeric 2-N- and 3-O-substituted isothiazolopyridines.[11]

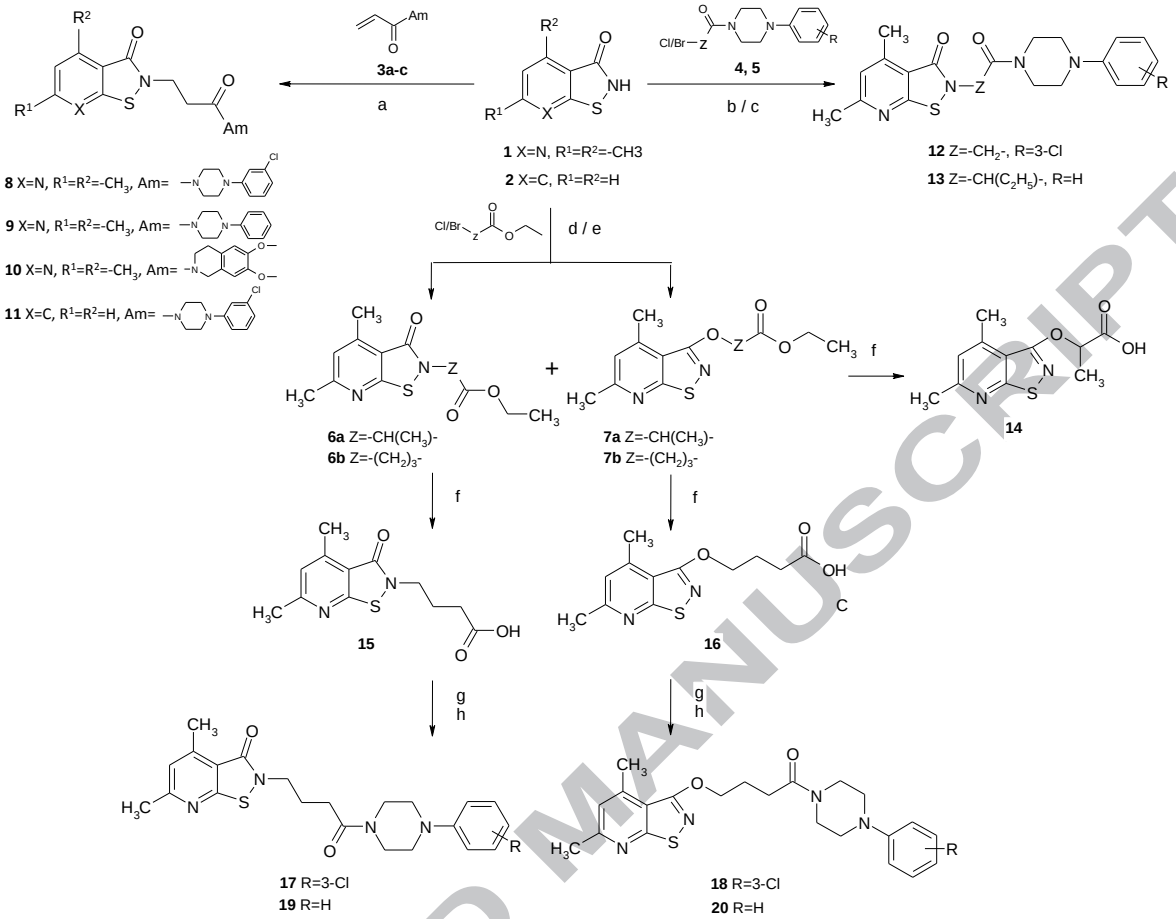

Scheme 1. Reagent and conditions: (a) toluene, reflux; (b) EtONa, anh. ethanol, reflux / (c) K_2CO_3, acetonitrile, reflux; (d) K_2CO_3, acetonitrile, reflux / (e) EtONa, DMF, reflux; (f) conc. HCl, reflux; (g) Et_3N, ethyl chloroformate, dichloromethane, 0°C; (h) 1-(3-chlorophenyl)piperazine/1-phenylpiperazine, room temp.

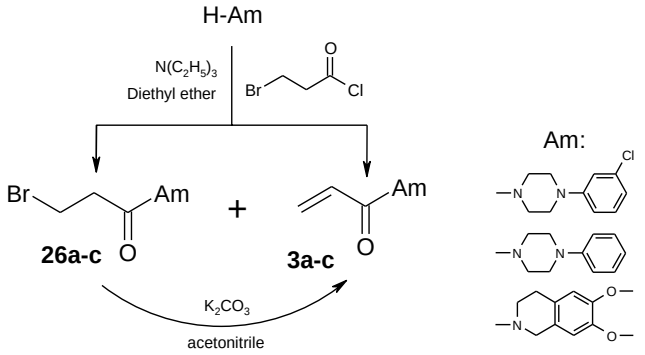

Scheme 2. Synthesis of compounds **3a-c** and **26a-c**.

2.2 IN VITRO CYCLOOXYGENASE (COX) INHIBITION ASSAY

Figure 2 shows the impact of piroxicam, the standard inhibitor of cyclooxygenases, on COX-1 and COX-2 activities at 2 min of incubation, as recommended for this test kit.

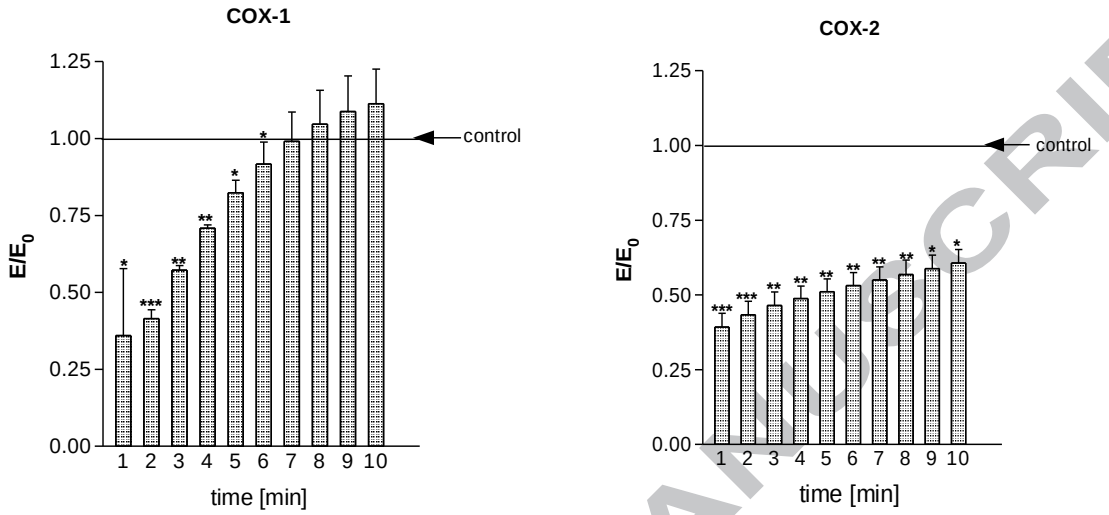

Figure 2. Impact of the model inhibitor piroxicam on COX-1 and COX-2 activity during the incubation period from 1 min to 10 min. Results obtained in samples with the tested drug were compared to those in the control cultures (the enzyme incubated without piroxicam; E_0), and the ratios of E/E_0 are given in Figure 2. Statistical significance was calculated with the t test (*p<0.05; **p0.01; ***p<0.001).

As can be seen in Figure 2, COX-1 activity markedly decreased within the first 6 min of incubation with piroxicam, even by 60-65% at 1 and 2 min. However, in the longer period, i.e. at 7-10 min, the inhibitory effect of the drug became weak and activity of the enzyme was even higher (although not statistically significant) than that in the control samples (the enzyme incubated without the tested drug). On the other hand, the decrease of COX-2 activity by piroxicam was significant within the whole period of incubation; when compared to relative control samples the (without the drug) the activity of COX-2 was decreased by 57% at 2 min and by 40% at 10 min.

The influence of the tested compounds on COX-1 and COX-2 activities at 2 min of incubation (fast impact) and at 10 min (persisting effect) was compared to the relative control samples (the enzyme activity without tested compounds) and is shown in Figures 3 and 4 as E/E_0 ratios. Statistical significance of the results was estimated with the paired *t* test.

Figure 3 presents the results of the COX-1 (A) and the COX-2 (B) activities estimated at 2 min of incubation with the tested compounds.

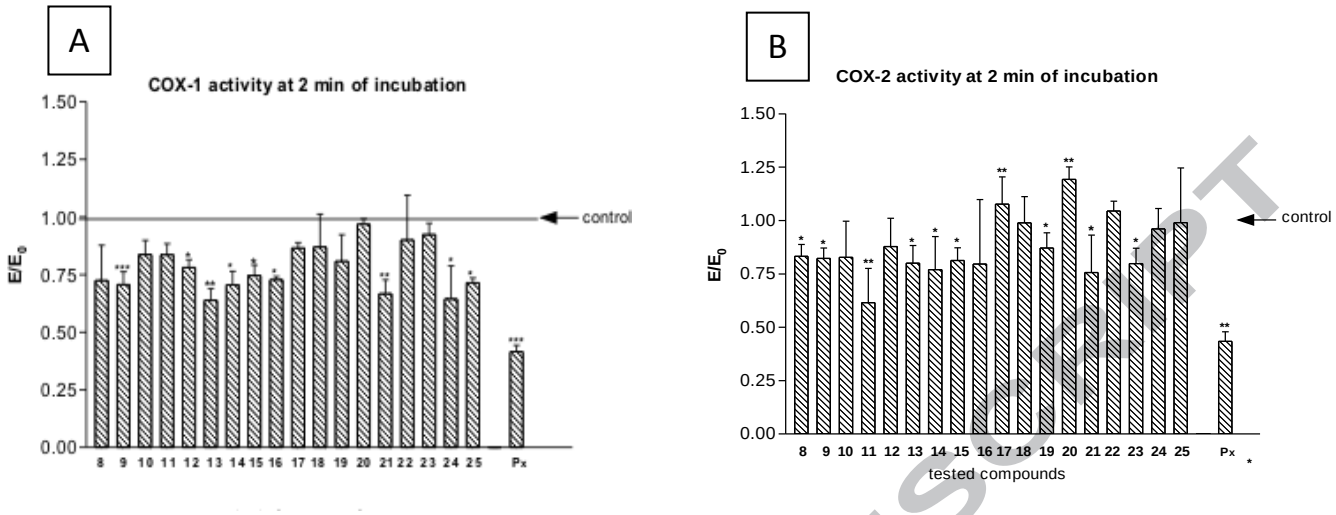

Figure 3. Activity of the COX-1 (A) and COX-2 (B) enzymes at 2 min of incubation with the tested compounds. Results were compared to relative control samples (without the tested compounds; E_0) and expressed as E/E_0 ratios. Statistical significance was calculated with the *t* test (*p<0.05; **p<0.01; ***p<0.001). The effect of the model cyclooxygenase inhibitor piroxicam (Px) was also estimated and is shown in the figure.

All the tested compounds inhibited the activity of COX-1 at 2 min after their addition, and the effect was the strongest in the cases of compounds 9, 13-16, 21 and 24 (inhibition of the enzyme by 25-40%).

Figure 3B reveals diverse effects of the tested compounds on COX-2. The enzyme's activity was strongly inhibited by compounds 11, 13-15, 21, 23 (by 20-25%), and, in contrast, was elevated in samples containing compounds 17 and 20 (by 7% and by 19%, respectively, when compared to the control samples).

The influence of the tested compounds on activity of both cyclooxygenases as estimated at 10 min of incubation is shown in Figure 4.

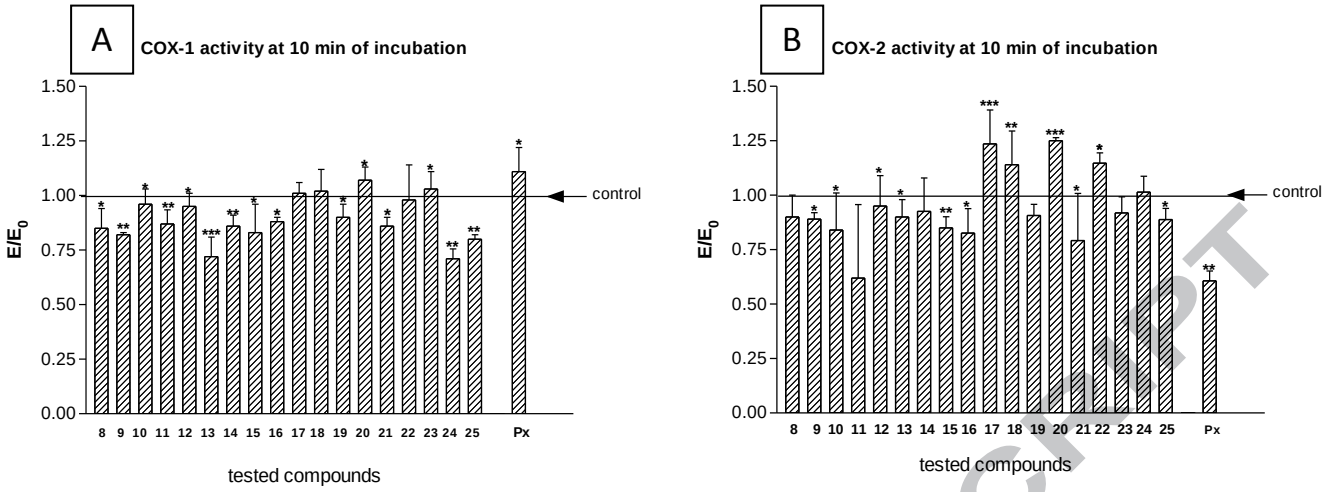

Figure 4. Activity of the COX-1 (A) and COX-2 (B) enzymes at 10 min of incubation with the tested compounds. Results were compared to relative control samples (without tested compounds; E_0) and expressed as E/E_0 ratios. Statistical significance was calculated with the *t* test (*p<0.05; **p<0.01; ***p<0.001). The effect of the model cyclooxygenase inhibitor piroxicam (Px) was also estimated and is shown in the figure.

As shown in Figure 4A, the activity of COX-1 was strongly inhibited during incubation with compounds 9, 13, 24 and 25 (by 18-30%). On the other hand, compounds 20 and 23 caused higher activity of the enzyme (3-7% higher than in the control). It should be noted that piroxicam enhanced COX-1 activity by 11% during 10 min of incubation.

Figure 4B demonstrates the diverse impact of the tested compounds on COX-2 activity at 10 min of incubation; both the inhibitory effect of compounds 15, 16, 21 and 25 (12-21%) and the stimulatory result of the enzyme's activity by compounds 17, 18, 20 and 22 (15-25%) were estimated. The inhibitory effect was the strongest in the case of compound 11 (38%). For comparison, the inhibitory effect of piroxicam was 40%.

Two-way analysis of variance confirmed that the tested compounds differed in their impact on cyclooxygenase activity ($F=19.78$, $df=35$, $p<10^{-4}$), and the impact on COX-1 and on COX-2 activity was markedly diverse ($F=86.72$, $df=1$, $p<10^{-4}$).

We calculated IC_{50} values (i.e. the concentration of tested compounds [μM] which can exert 50% inhibition of the enzyme activity), separately with COX-1 and COX-2 activity estimations at 2 min of incubation with the tested compounds. Selectivity of the compounds to COX-1 or to COX-2 was assessed by calculation of the IC_{50} ratios. The IC_{50} values were not calculated with those tested compounds which exerted very low inhibitory activity at 2 min of incubation. The results of the calculation are given in Table 1.

Table 1. IC_{50} values (SD) calculated for COX-1 and COX-2 activities at 2 min of incubation with the tested compounds [mean (SD); n=3].

Compound	IC_{50} [μM] (SD)		Ratio: COX-2/COX-1
	COX-1	COX-2	
8	241.9 (10.4)	388.0 (8.8)	1.60
9	206.6 (2.2)	368.2 (4.2)	1.78
10	497.3 (9.7)	303.4 (16.0)	0.61
11	330.6 (5.3)	129.9 (27.7)	0.39
12	374.6 (5.0)	605.1 (22.4)	1.61
13	153.6 (3.9)	343.6 (9.4)	2.24
14	229.1 (3.8)	326.9 (22.8)	1.43
15	235.2 (6.1)	302.3 (4.9)	1.28
16	248.4 (1.5)	269.0 (26.5)	1.08
17	722.3 (7.2)	-	-
18	818.2 (26.5)	-	-
19	349.2 (10.3)	459.0 (7.4)	1.31
20	-	-	-
21[14]	210.5 (3.0)	222.6 (24.3)	1.06
22[11]	815.6 (39.1)	-	-
23[12]	-	358.8 (7.8)	-
24[12]	156.4 (8.4)	-	-
25[12]	218.9 (2.5)	494.3 (14.9)	2.26
Piroxicam	254.6 (6.5)	102.8 (2.2)	0.40

Data on the ratios of COX-2 to COX-1 activity included in Table 1 clearly indicate those compounds which exerted significant COX-1 selectivity (13 and 25) and COX-2 preferences (10 and 11). However, compounds 16 and 21 exhibited almost equally strong inhibitory action on COX-1 and COX-2 activities.

These compounds should be further studied in terms of their selectivity and balanced inhibitory action on cyclooxygenases as candidates for new anti-inflammatory drugs.

2.3 STRUCTURE-BASED STUDIES

2.3.1 MOLECULAR MODELING STUDIES

In the present study 18 new inhibitors were tested. Every compound was synthesized and biological activity was determined as described in the materials and methods section. Additionally, a molecular docking study was calculated to evaluate the mode of binding for the compounds. The docking results and biological activity expressed as pIC_{50} are presented in Table 2. The full list of results is available in Table S1 in the supporting materials.

Currently, almost 70 crystal structures of cyclooxygenases are deposited in the Protein Data Bank. For most of them the high-resolution crystal structure co-crystallized with ligand(s) is available. It allows extensive investigation of the binding mode for potential inhibitors.

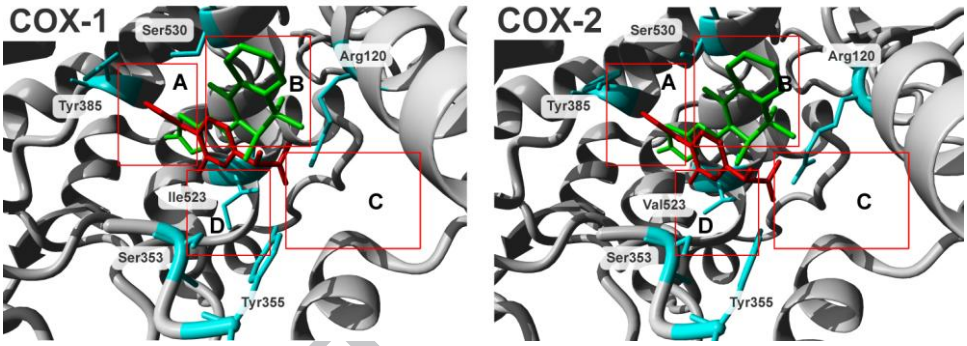

Figure 5. Illustration of four characteristic subdomains of the COX enzyme ligand binding domain, indicated by red boxes A, B, C and D.

Here, the authors specified in the COX ligand binding domain four characteristic subdomains of the enzyme (Figure 5, red boxes A, B, C and D). The subdomains represent pockets where the native substrate (arachidonic acid) as well as the enzyme inhibitors may potentially bind. Two of the inhibitors (flurbiprofen and meloxicam) representing high biological activity (pIC_{50} = 5.7 – 8 for flurbiprofen[16] and COX-1 pIC_{50} = 6; COX-2 pIC_{50} = 6.82 for meloxicam[17]) were shown to characterize the subdomains. Subdomain A represents the mode of binding of flurbiprofen, subdomain B represents the mode of binding of meloxicam, subdomain C represents an entrance region of the enzyme binding domain, and subdomain D represents the position of the residue in position 523: the isoleucine in COX-1 and the valine in COX-2. Position 523 is the main cluster of differentiation between COX-1

and COX-2 active sites, being the main target for selective compounds. The smaller Val523 residue in COX-2 allows access to a hydrophobic side-pocket in the enzyme which Ile523 sterically hinders.[18] In terms of their molecular biology, COX-1 and COX-2 are of similar molecular weight, approximately 70 and 72 kDa, respectively. The enzymes have near-identical catalytic sites although their amino acid sequence homology is only 65%, which implies a slightly different mode of binding for the same compounds under COX-1 and COX-2 binging conditions, as described in the example of meloxicam elsewhere.[18-20] To correlate mode of binding with biological activity, the compounds were docked to the appropriate crystal structures and evaluated by scoring function.

Table 2. Selected docking results sorted by biological activity for COX-1 and COX-2.

COX-1			COX-2		
Compound	pIC_{50}	MolDock Score	Compound	pIC_{50}	MolDock Score
13	3.86	-94.8466	**11**	3.89	-248.91
21[14]	3.82	-91.3921	**21**[14]	3.69	-167.797
25[12]	3.76	-81.7048	**13**	3.6	-206.268
11	3.52	-106.809	**25**[12]	2.28	-215.663

2.3.2 GENERAL MODE OF BINDING

As reported previously, induced fit and dissociation times are the most important components reflecting biological activity in the case of enzyme inhibition.[17,24] In general, this observation explains the behavior of the presented compounds and their biological activity. Due to high homology between COX-1 and COX-2 binding domains for almost all of the compounds, observed interactions with both binding domains are quite similar, which is also reflected when average activities COX-1 pIC_{50} = 3.58 and COX-2 pIC_{50} = 3.37 are compared. In general, the bulky compounds (8-13, 17-20, 22-25) bind to the enzyme by the phenylpiperazine rings to internal part of the COX-1 and COX-2 enzyme (Figure 6, red box A) and the isothiazolopyridine/benzisothiazole rings directed to the opposite site (Figure 6, red box C). This type of binding in the example of compound 13 (Figure 6, blue compound) is observed for almost all of the bulky compounds, except compound 11 under COX-2 binding conditions.

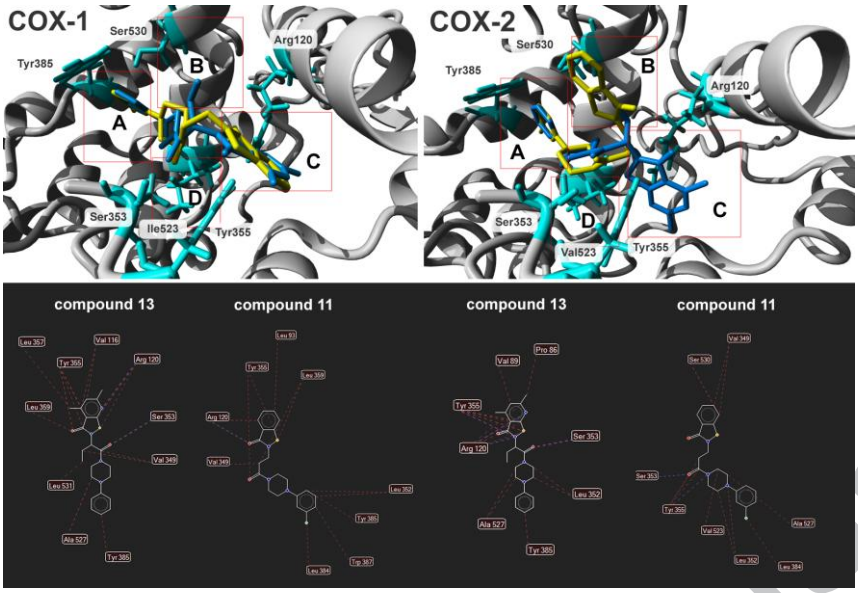

Figure 6. Docking poses of 13 (light blue) and 11 (yellow) under COX-1 and COX-2 binding domain conditions (top panel) and ligand maps representing interactions by hydrogen bonds (blue dot line) and steric interactions (red dot line) (bottom panel). Residues colored cyan; all hydrogens were hidden. A, B, C, D – binding subdomains; details in the text.

As presented in Table 2, when compounds are compared by biological activity the most potent compounds are 13 in the group of COX-1 and 11 in the group of COX-2. As can be observed, both compounds bind by the phenylpiperazine rings to the internal part of the COX-1 and COX-2 enzyme (Figure 6, red box A). In both cases, the phenylpiperazine rings are in a similar position as represented by flurbiprofen (supporting materials, Figure S1, red compound). The isothiazolopyridine/benzisothiazole rings are directed to the opposite site (referring to the phenylpiperazine ring) representing an entrance region of the enzyme binding domain (Figure 6, red box C). Compound 13 occupies almost the same position under COX-1 and COX-2 binding conditions opposite to 11, which is similar to position 13 under COX-1 and quite different in the case of COX-2. It can be observed that the benzisothiazole ring of 11 occupies subdomain B, which represents the meloxicam mode of binding (supporting materials, Figure S1, green compound). An explanation of this behavior is the difference between COX-1 and COX-2 binding domains in position 523. The smaller valine residue in COX-2 (Figure 6, red box D) compared to isoleucine in COX-1 (Figure 6, red box D) allows access to a hydrophobic side-pocket in the enzyme.[18] Due to higher obtained activity of 13 (pIC_{50} = 3.86) compared to 11 (pIC_{50} = 3.52) under COX-1 owing to the ethyl group in position X' it sterically interacts with the meloxicam-like binding domain (Figure 6, red box B). Also, the ethyl group is important for 13 under COX-2 (pIC_{50} = 3.6), although the 11

benzisothiazole ring system goes deeper into the domain, which increases activity (pIC_{50} = 3.89) and prevents too early dissociation. This small pocket in the COX-2 active site admits compound 11 to bend and access by the benzisothiazole rings a similar domain as the meloxicam benzothiazine rings (Figure 6, red box B). Additionally, compounds 13 and 11 interact with the binding domain by hydrogen bonds. Compound 13 interacts with COX-1 by arginine 120 (Arg 120) and serine 353 (Ser 353) and with COX-2 by tyrosine 355 (Tyr 355), arginine 120 (Arg 120) and serine 353 (Ser 353). Compound 11 interacts with COX-1 by arginine 120 (Arg 120) and with COX-2 by serine 353 (Ser 353) and tyrosine 355 (Tyr 355), as shown in Figure 6, bottom panel.

For the other compounds, the biological activity is a direct result of the dissociation time from the binding domain, which is a composition of two components: the length of the linker and steric fit to the external domain more dissimilar between enzyme variants. The general correlation between binding mode and observed biological activity might be explained by considering the group of compounds 17, 20 and 22. Compounds 17, 20 and 22 are presented in Figure 7 as green, violet and red, respectively. The compounds are biologically active under COX-1 and inactive under COX-2 binding conditions. The general mode of binding for both groups is almost the same, with the difference that the compounds under COX-1 may occupy an external hydrophobic domain which is lost under COX-2. Even though the compounds under COX-2 penetrate the domain deeper, their steric anchor is less powerful and the compounds dissociate faster. This observation correlates with biological activity pIC_{50} = 3.28, 3.43, 2.81 for 22, 17, 20, respectively.

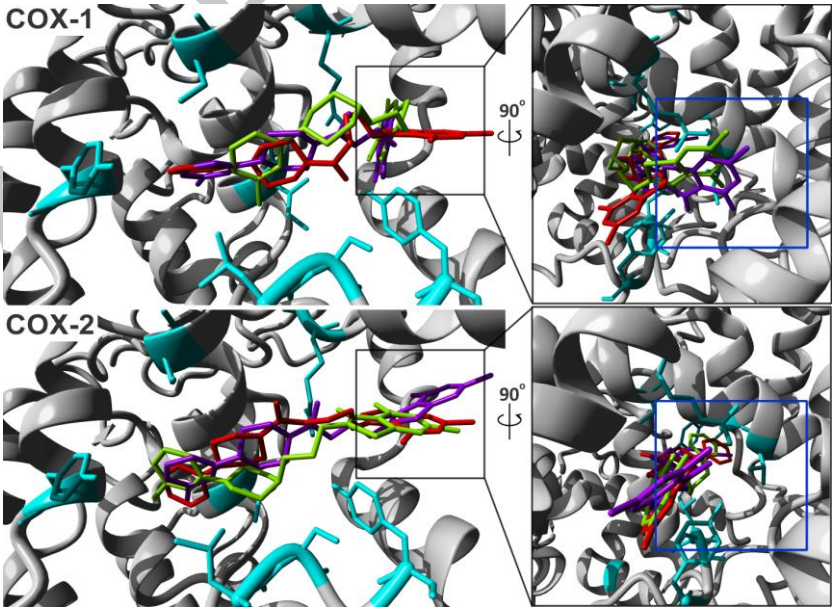

Figure 7. Docking poses of 22 (green), 17 (violet) and 20 (red) under COX-1 and COX-2 binding domain conditions (left panel) and the same docking positions from the binding domain entrance perspective (right panel). Residues colored cyan; all hydrogens were hidden. A, B, C, D – binding subdomains; details in the text.

2.3.3 COMPOUNDS' SELECTIVITY

The small compounds (14-16, 21) bind to the central part of the catalytic domain. As presented in the example of 21 (Figure 8, magenta), it shares almost the same position as flurbiprofen (Figure S1 in supporting materials) and its selectivity is slight (21, Δ pIC_{50} = 0.13). Higher selectivity might be observed for compound 11 in the case of COX-2 (Δ pIC_{50} = 0.29) and 13 in the case of COX-1 (Δ pIC_{50} = 0.34). However, the highest selectivity is observed for compound 25 (Δ pIC_{50} = 1.48), due to compound 25 binding in a slightly different manner compared to 21 (Figure 8, magenta). It resembles compound 11's mode of binding under COX-2 binding conditions. In the case of 25 the isoleucine 523 residue in COX-1 sterically stabilizes the compound in the binding domain, and this steric promoter is lost when valine 523 is under the COX-2 binding domain (Figure 8, ligand map with red dotted line). Compound 25 stabilized by isoleucine stays longer in the binding domain, which is directly reflected in biological activity.

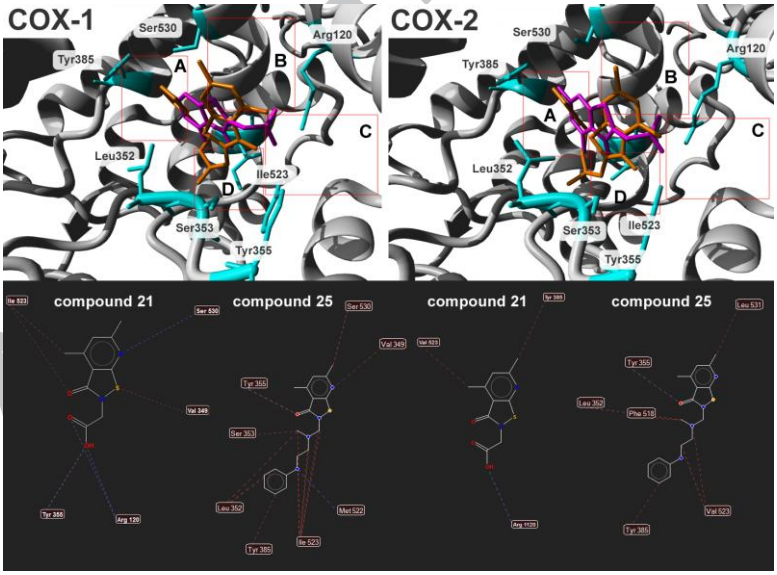

Figure 8. Docking poses of 21 (light blue) and 25 (yellow) under COX-1 and COX-2 binding domain conditions (top panel) and ligand maps representing interactions by hydrogen bonds (blue dotted line) and steric interactions (red dotted line) (bottom panel). Residues colored cyan; all hydrogens were hidden. A, B, C, D – binding subdomains; details in the text.

Additionally, the Schrödinger atom-based QSAR, CoMFA and CoMSIA models were determined, but they did not provide any further insight for the discussion.

3. CONCLUSION

Here, we have presented the previously unexplored isothiazolopyridine scaffold as a COX inhibitor and its phenylpiperazine derivatives connected by different linkers.

All the tested compounds inhibited the activity of COX-1 at 2 min after addition of the tested compounds. This effect was the strongest in the cases of compounds 9, 13-16, 21 and 24 (inhibition of the enzyme by 25-40%). The COX-2 enzyme's activity was strongly inhibited by compounds 11, 13-15, 21 and 23 (by 20-25%).

Activity of COX-1 was strongly inhibited during 10 min incubation with compounds 9, 13, 24 and 25 (by 18-30%). On the other hand, compounds 20 and 23 caused higher activity of the enzyme (by 3-7% as high as in the relative control). It should be noted that piroxicam enhanced COX-1 activity by 11% during 10 min of incubation. The diverse impact of the tested compounds on the COX-2 activity at 10 min of incubation was observed. The inhibitory effect of compounds 15, 16, 21 and 25 (by 12-21%) and the stimulatory effect of the enzyme's activity by compounds 17, 18, 20 and 22 (by 15-25%) were noted. The inhibitory effect was the strongest in the case of compound 11 (by 38%). For comparison, the inhibitory effect of piroxicam was 40%.

Data on the ratios of COX-2 to COX-1 activity clearly indicate those compound which showed significant COX-1- (13 and 25) and COX-2- (10 and 11) selectivity. However, compounds 16 and 21 exhibited almost equally strong inhibitory action on COX-1 and COX-2 activities.

These compounds should be further studied in terms of their selectivity or balanced inhibitory action on cyclooxygenases as candidates for new anti-inflammatory drugs.

The smallest acetic acid derivative of the proposed scaffold (21) showed a similar mode of binding as flurbiprofen from the crystal structure and similar activity as piroxicam.

4. EXPERIMENTAL SECTION

4.1. Chemistry

All chemicals used were purchased from commercial suppliers. Dry solvents were obtained according to the standard procedure. Progress of the reaction was monitored by TLC on silica gel 60 F254-coated TLC plates (Fluka Chemie GmbH) and visualized by UV light at 254 nm.

Flash column chromatographic purifications were performed using Sigma-Aldrich 60A silica gel 230–400 mesh. The proton nuclear magnetic resonance (^{1}H NMR) spectra were recorded on a Bruker 300 MHz NMR spectrometer in *d*-chloroform ($CDCl_3$) or d_6-dimethylsulfoxide (DMSO-d_6) and tetramethylsilane (TMS) was used as an internal reference. Chemical shifts are given in ppm units, and coupling constant values are given in Hz. Infrared (IR) spectra were run on a Perkin-Elmer Spectrum Two UATR FT-IR spectrometer, and frequencies are reported in cm^{-1}. The samples were applied as solids. Elemental analyses for carbon, nitrogen and hydrogen were carried out on a Carlo Erba NA 1500 analyser and were within ±0.4 % of the theoretical value.

4.1.1. General method for preparation of 2-(3-oxo-3-substituted-propyl)-4,6-dimethylisothiazolo[5,4-*b*]pyridin-3(2*H*)-one/1,2-benzisothiazol-3(2*H*)-one derivatives (8-11) (Scheme 1)

4.1.1.1. Acrylamide (3a-c) and 3-bromopropanamide (26a-c) derivatives (Scheme 2)

5 mmol of the appropriate amine derivative [1-(3-chlorophenyl)piperazine to obtain **3a** and **26a**, 1-phenylpiperazine to obtain **3b** and **26b**, 6,7-dimethoxy-1,2,3,4-tetrahydroisoquinoline to obtain **3c** and **26c**] was dissolved in 30 mL of diethyl ether with addition of 5 mmol triethylamine and stirred slowly at room temperature for 10 minutes. Then 5 mmol of 3-bromopropionyl chloride in 10 mL of diethyl ether was slowly instilled and stirring was continued for another 1 hours. After this time diethyl ether was evaporated in a vacuum, 10 mL of water and 60 mL of chloroform were added, and the mixture was separated in a funnel into two parts. The chloroform part was dried with magnesium sulfate and evaporated in a vacuum. The resulting residue was chromatographed, and obtained compounds were used in the subsequent reactions without further purification.

4.1.1.1.1. 1-acryloyl-4-(3-chlorophenyl)piperazine (3a)

Anal. $C_{13}H_{15}ClN_2O$ (m.w. 250.72); CC (ethyl acetate, R_f=0.57), m.p. 69-71˚C, FT-IR (UATR, selected lines) ν_{max}/cm^{-1}: 1655 (C=O), 1680 (C=C), 3085 (=C-H). ^{1}H NMR ($CDCl_3$) δ: 3.18-3.22 (t, 4H, 2x$CH_{2\text{-piperazine}}$, *J*=5.1), 3.72-3.84 (m, 4H, 2x$CH_{2\text{-piperazine}}$), 5.72 (dd, 1H, CH_2=CH, *J*=2.1 and *J*=10.5 Hz), 6.30 (dd, 1H, CH_2=CH, *J*=1.8 and *J*=16.8 Hz), 6.55 (dd, 1H, CH_2=CH, *J*=10.5 and *J*=16.8 Hz), 6.88-7.31 (m, 5H, ArH).

4.1.1.1.2. 1-acryloy-4-phenylpiperazine (3b)

Anal. $C_{13}H_{16}N_2O$ (m.w. 216.29); CC (ethyl acetate, R_f=0.53), m.p. 63-65˚C, FT-IR (UATR, selected lines) ν_{max}/cm^{-1}: 1650 (C=O), 1675 (C=C), 3080 (=C-H).^{1}H NMR ($CDCl_3$) δ: 3.18-

3.21 (t, 4H, 2x$CH_{2\text{-piperazine}}$, *J*=5.1), 3.72-3.85 (m, 4H, 2x$CH_{2\text{-piperazine}}$), 5.71 (dd, 1H, CH_2=CH, *J*=1.8 and *J*=10.5 Hz), 6.29 (dd, 1H, CH_2=CH, *J*=1.8 and *J*=16.8 Hz), 6.56 (dd, 1H, CH_2=CH, *J*=10.5 and *J*=16.8 Hz), 6.77-7.16 (m, 4H, ArH).

4.1.1.1.3. 2-acryloyl-6,7-dimethoxy-1,2,3,4-tetrahydroisoquinoline (3c)

Anal. $C_{14}H_{17}NO_3$ (m.w. 247.30); CC (ethyl acetate, R_f=0.43), m.p. 99-101˚C, FT-IR (UATR, selected lines) ν_{max}/cm^{-1}: 1655 (C=O), 1680 (C=C), 3060 (=C-H). ^{1}H NMR ($CDCl_3$) δ: 2.79-2.85 (m, 2H, $CH_{2\text{-tetrahydroisoquinoline}}$), 3.74-3.78 (m, 2H, $CH_{2\text{-tetrahydroisoquinoline}}$), 3.85 (s, 6H, 2x$CH_3$O), 4.65 (s, 0.75H, $CH_{2\text{-tetrahydroisoquinoline}}$), 4.72 (s, 1.25H, $CH_{2\text{-tetrahydroisoquinoline}}$), 5.70 (dd, 1H, CH_2=CH, *J*=1.8 and *J*=10.5 Hz), 6.29 (dd, 1H, CH_2=CH, *J*=1.8 and *J*=16.8 Hz), 6.57-6.69 (m, 3H, CH_2=CH + 2xArH).

4.1.1.1.4. 1-(3-bromopropanoyl)-4-(3-chlorophenyl)piperazine (26a)

Anal. $C_{13}H_{16}BrClN_2O$ (m.w. 331.64); CC (ethyl acetate, R_f=0.75), m.p. 78-80˚C, FT-IR (UATR, selected lines) ν_{max}/cm^{-1}: 1650 (C=O). ^{1}H NMR ($CDCl_3$) δ: 2.97 (t, 2H, CH_2CO, *J*=7.2 Hz), 3.17-3.23 (m, 4H, 2x$CH_{2\text{-piperazine}}$), 3.63-3.83 (m, 6H, 2x$CH_{2\text{-piperazine}}$ + $BrCH_2$), 6.81-7.23 (m, 4H, ArH).

4.1.1.1.5. 1-(3-bromopropanoyl)-4-phenylpiperazine (26b)

Anal. $C_{13}H_{17}BrN_2O$ (m.w. 297.20); CC (ethyl acetate, R_f=0.72), m.p. 73-76˚C, FT-IR (UATR, selected lines) ν_{max}/cm^{-1}: 1660 (C=O). ^{1}H NMR ($CDCl_3$) δ: 2.95 (t, 2H, CH_2CO, *J*=7.2 Hz), 3.15-3.21 (m, 4H, 2x$CH_{2\text{-piperazine}}$), 3.64-3.86 (m, 6H, 2x$CH_{2\text{-piperazine}}$ + $BrCH_2$), 6.89-7.30 (m, 5H, ArH).

4.1.1.1.6. 2-(3-bromopropanoyl)-6,7-dimethoxy-1,2,3,4-tetrahydroisoquinoline (26c)

Anal. $C_{14}H_{18}BrNO_3$ (m.w. 327.9); CC (ethyl acetate, R_f=0.62), m.p. 80-84˚C, FT-IR (UATR, selected lines) ν_{max}/cm^{-1}: 1645 (C=O).^{1}H NMR ($CDCl_3$) δ: 2.77-3.02 (m, 4H, $CH_{2\text{-tetrahydroisoquinoline}}$ + CH_2CO), 3.64-3.71 (m, 2H, $BrCH_2$), 3.81-3.86 (m, 8H, $CH_{2\text{-tetrahydroisoquinoline}}$ + 2xCH_3O), 4.55 (s, 0.75H, $CH_{2\text{-tetrahydroisoquinoline}}$), 4.66 (s, 1.25H, $CH_{2\text{-tetrahydroisoquinoline}}$), 6.58-6.62 (m, 2H, ArH).

4.1.1.2. Dehydrohalogenation of 3-bromopropanamide derivatives to the corresponding acrylamides (Scheme 2)

A mixture of 5 mmol of corresponding 3-bromopropanamides and 5 mmol of anhydrous potassium carbonate in 30 mL of acetonitrile was refluxed with stirring for 10 h. The hot reaction mixture was filtered and evaporated to dryness to give appropriate acrylamides.

4.1.1.3. 2-(3-oxo-3-substituted-propyl)-4,6-dimethylisothiazolo[5,4-*b*]pyridin-3(2*H*)-one/1,2-benzisothiazol-3(2*H*)-one derivatives (8-11) (Scheme 1)

A mixture of 4,6-dimethylisothiazolo[5,4-*b*]pyridin-3(2*H*)-one **1** or 1,2-benzisothiazol-3(2*H*)-one **2** (3 mmol) with 3 mmol of corresponding acrylamide derivatives in 30 mL of toluene was refluxed with stirring for 8 h. After this time the mixture was evaporated to dryness. The product was isolated from the resulting residue by column chromatography (ethyl acetate) and purified by crystallization from appropriate solvents.

4.1.1.3.1. 2-{3-oxo-3-[4-(3-chlorophenyl)piperazin-1-yl]propyl}-4,6-dimethylisothiazolo[5,4-*b*]pyridin-3(2*H*)-one (8)

Anal. $C_{21}H_{23}ClN_4O_2S$ (m.w. 430.96); CC (ethyl acetate, R_f=0.37), 67% yield, m.p. 141-143˚C (methanol). FT-IR (UATR, selected lines) ν_{max}/cm^{-1}: 1670 (3-C=O), 1640 (amide C=O). ^{1}H NMR ($CDCl_3$) δ: 2.58 (s, 3H, $CH_{3\text{-pyridine}}$), 2.73 (s, 3H, $CH_{3\text{-pyridine}}$), 2.84 (t, 2H, CH_2CON, J=6.6 Hz), 3.13-3.16 (m, 4H, 2x$CH_{2\text{-piperazine}}$), 3.59 (t, 2H, $CH_{2\text{-piperazine}}$, J=5.1 Hz), 3.78 (t, 2H, $CH_{2\text{-piperazine}}$, J=5.1 Hz), 4.20 (t, 2H, $N_{isothiazole}$-CH_2, J=6.6 Hz), 6.74-7.20 (m, 5H, $H_{\beta\text{-pyridine}}$ + 4ArH). ^{13}C NMR ($CDCl_3$) δ: 17.55 (CH_3), 24.05 (CH_3), 32.54 (CH_2), 40.18 ($C_{\text{-piperazine}}$), 41.35 ($C_{\text{-piperazine}}$), 45.01 (CH_2), 49.12 ($C_{\text{-piperazine}}$), 49.35 ($C_{\text{-piperazine}}$), 114.73 ($C_{\text{-pyridine}}$), 115.41 (C-$_{Ar}$), 116.64 (C-$_{Ar}$), 117.46 (C-$_{Ar}$), 118.84 (C-$_{Ar}$), 120.70 (C-$_{Ar}$), 123.10 (C-$_{Ar}$), 127.44 ($C_{\text{-pyridine}}$), 137.35 ($C_{\text{-pyridine}}$), 142.26 ($C_{\text{-pyridine}}$), 151.46 ($C_{\text{-pyridine}}$), 164.55 (CO), 168.47 (CO). *Anal. Calcd*: C, 58.52; H, 5.39; N, 13.00. *Found:* C, 58.70; H, 5.55; N, 12.86.

4.1.1.3.2. 2-[3-oxo-3-(4-phenylpiperazin-1-yl)propyl]-4,6-dimethylisothiazolo[5,4-*b*]pyridin-3(2*H*)-one (9)

Anal. $C_{21}H_{24}N_4O_2S$ (m.w. 396.52); CC (ethyl acetate, R_f=0,33), 45% yield, m.p. 124-126˚C (ethanol). FT-IR (UATR, selected lines) ν_{max}/cm^{-1}: 1670 (3-C=O), 1640 (amide C=O). ^{1}H NMR ($CDCl_3$) δ: 2.58 (s, 3H, $CH_{3\text{-pyridine}}$), 2.73 (s, 3H, $CH_{3\text{-pyridine}}$), 2.85 (t, 2H, CH_2CON, J=6.6 Hz), 3.14-3.18 (m, 4H, 2x$CH_{2\text{-piperazine}}$), 3.64 (t, 2H, $CH_{2\text{-piperazine}}$, J=5.1 Hz), 3.82 (t, 2H, $CH_{2\text{-piperazine}}$, J=5.1 Hz), 4.20 (t, 2H, $N_{isothiazole}$-CH_2, J=6.6 Hz), 6.92-7.31 (m, 6H, $H_{\beta\text{-pyridine}}$ + 5ArH). *Anal. Calcd*: C, 63.61; H, 6.10; N, 14.13. *Found:* C, 63.50; H, 6.42; N, 14.07.

4.1.1.3.3. 2-[3-oxo-3-(6,7-dimethoxy-3,4-dihydroisoquinolin-2(1*H*)-yl)propyl]-4,6-dimethylisothiazolo[5,4-*b*]pyridin-3(2*H*)-one (10)

Anal. $C_{22}H_{25}N_3O_4S$ (m.w. 427.53); CC (ethyl acetate, R_f=0.16), 49% yield, m.p. 144-145˚C (methanol). FT-IR (UATR, selected lines) ν_{max}/cm^{-1}: 1670 (3-C=O), 1640 (amide C=O). ^{1}H NMR ($CDCl_3$) δ: 2.59-2.79 (m, 8H, 2x$CH_{3\text{-pyridine}}$ + $CH_{2\text{-tetrahydroisoquinoline}}$), 2.87 (q, 2H, CH_2CON, J=6,3 Hz), 3.61-3.65 (t, 1H, $CH_{2\text{-tetrahydroisoquinoline}}$, J=6.0 Hz), 3.80-3.85 (m, 7H, $CH_{2\text{-tetrahydroisoquinoline}}$ + 2xCH_3O), 4.20 (q, 2H, $N_{isothiazole}$-CH_2, J=6.6 Hz), 4,49 (s, 1H, CH_2-

$_{\text{tetrahydroisoquinoline}}$), 4.67 (s, 1H, $CH_{2\text{-tetrahydroisoquinoline}}$), 6.44-6.93 (m, 3H, $H_{\beta\text{-pyridine}}$ + 2ArH). *Anal. Calcd*: C, 61.81; H, 5.89; N, 9.83. *Found:* C, 62.10; H, 6.12; N, 9.64.

4.1.1.3.4. 2-{3-oxo-3-[4-(3-chlorophenyl)piperazin-1-yl]propyl}-1,2-benzisothiazol-3(2*H*)-one (11)

Anal. $C_{20}H_{22}ClN_3O_2S$ (m.w. 401.91); CC (ethyl acetate, R_f=0.41), 32% yield, m.p. 131-133˚C (ethanol). FT-IR (UATR, selected lines) ν_{max}/cm^{-1}: 1710 (3-C=O), 1640 (amide C=O). ^{1}H NMR ($CDCl_3$) δ: 2.85 (t, 2H, CH_2CON, J=6.3 Hz), 3.09-3.15 (m, 4H, $2xCH_{2\text{-piperazine}}$), 3.58 (t, 2H, $CH_{2\text{-piperazine}}$, J=5.4 Hz), 3.77 (t, 2H, $CH_{2\text{-piperazine}}$, J=5.4 Hz), 4.22 (t, 2H, $N_{\text{isothiazole-}}CH_2$, J=6.3 Hz), 6.73-7.99 (m, 8H, ArH). *Anal. Calcd*: C, 59.76; H, 5.03; N, 10.46. *Found:* C, 60.14; H, 5.24; N, 10.39.

4.1.2. Method for the synthesis of 2-{2-oxo-2-[4-(3-chlorophenyl)piperazin-1-yl]ethyl}-4,6-dimethylisothiazolo[5,4-*b*]pyridin-3(2*H*)-one (12) (Scheme 1)

4.1.2.1. 1-chloroacetyl-4-(3-chlorophenyl)piperazine (4)

Compound **4** was prepared according to the procedure described in **4.1.1.1.**, starting from 1-(3-chlorophenyl)piperazine and equimolar amounts of chloroacetyl chloride. The oily residue was chromatographed (CC, ethyl acetate).

Anal. $C_{12}H_{14}Cl_2N_2O$ (m.w. 273.16); FT-IR (UATR, selected lines) ν_{max}/cm^{-1}: 1655 (C=O). ^{1}H NMR ($CDCl_3$) δ: 3.18-3.27 (m, 4H, $2xCH_{2\text{-piperazine}}$), 3.71 (t, 2H, $CH_{2\text{-piperazine}}$, J=5.1 Hz), 3.81 (t, 2H, $CH_{2\text{-piperazine}}$, J=5.1 Hz), 4.11 (s, 2H, CH_2CO), 6.92-7.33 (m, 4H, ArH).

4.1.2.2. 2-{2-oxo-2-[4-(3-chlorophenyl)piperazin-1-yl]ethyl}-4,6-dimethylisothiazolo[5,4-*b*]pyridin-3(2*H*)-one (12)

To the solution of sodium ethoxide, prepared from 0.23 g of Na and 50 mL of anh. ethanol, 2 mmol of 4,6-dimethylisothiazolo[5,4-*b*]pyridin-3(2*H*)-one **1** and 3 mmol of 1-chloroacetyl-4-(3-chlorophenyl)piperazine **4** were added. The mixture was refluxed with stirring for 5 h. After this time the mixture was cooled, then the precipitated product was filtered off, washed with water and crystallized from methanol.

Anal. $C_{20}H_{21}ClN_4O_2S$ (m.w. 416.93); 47% yield, m.p. 144-146˚C. FT-IR (UATR, selected lines) ν_{max}/cm^{-1}: 1650 (3-C=O and amide C=O). ^{1}H NMR ($CDCl_3$) δ: 2.67 (s, 3H, $CH_{3\text{-pyridine}}$), 2.79 (s, 3H, $CH_{3\text{-pyridine}}$), 3.22-3.26 (m, 4H, $2xCH_{2\text{-piperazine}}$), 3.75 (t, 2H, $CH_{2\text{-piperazine}}$, J=5.1 Hz), 3.82 (t, 2H, $CH_{2\text{-piperazine}}$, J=5.1 Hz), 4.70 (s, 2H, $N_{\text{isothiazole-}}CH_2$), 6.84-7.18 (m, 5H, $H_{\beta\text{-pyridine}}$ + 4ArH). *Anal. Calcd*: C, 57.62; H, 5.08; N, 13.44. *Found:* C, 57.24; H, 5.17; N, 13.25.

4.1.3. Method for the synthesis of 2-[1-oxo-1-(4-phenylpiperazin-1-yl)butan-2-yl]-4,6-dimethylisothiazolo[5,4-*b*]pyridin-3(2*H*)-one (13) (Scheme 1)

4.1.3.1. 1-(2-bromobutanoyl)-4-phenylpiperazine (5)

Compound **5** was prepared according to the procedure described in **4.1.1.1.**, starting from 1-phenylpiperazine and equimolar amounts of 2-bromobutyryl bromide. The oily residue was chromatographed (CC, ethyl acetate, R_f=0.86).

Anal. $C_{14}H_{19}BrN_2O$ (m.w. 311.22); FT-IR (UATR, selected lines) ν_{max}/cm^{-1}: 1660 (C=O). ^1H NMR ($CDCl_3$) δ: 1.02-1.08 (m, 3H, CH_3CH_2), 2.02-2.24 (m, 2H, CH_3CH_2), 3.25-3.28 (m, 4H, 2x$CH_{2\text{-piperazine}}$), 3.70-3.97 (m, 4H, 2x$CH_{2\text{-piperazine}}$), 4.35 (t, 1H, CH_2CH(Br)CO, J=7.2 Hz), 6.91-7.33 (m, 5H, ArH).

4.1.3.2. 2-[1-oxo-1-(4-phenylpiperazin-1-yl)butan-2-yl]-4,6-dimethylisothiazolo[5,4-*b*]pyridin-3(2*H*)-one (13)

A mixture of 5 mmol of 4,6-dimethylisothiazolo[5,4-*b*]pyridin-3(2*H*)-one **1**, 5 mmol of anhydrous potassium carbonate and 5.5 mmol of 1-(2-bromobutanoyl)-4-phenylpiperazine **5** in acetonitrile (30 mL) was refluxed for 4 h. The hot reaction mixture was filtered and evaporated to dryness. The product was isolated from the resulting residue by column chromatography (ethyl acetate/cyclohexane/chloroform 2:2:1) and purified by crystallization from methanol.

Anal. $C_{22}H_{26}N_4O_2S$ (m.w. 410.54); 44% yield, m.p. 121-124˚C. FT-IR (UATR, selected lines) ν_{max}/cm^{-1}: 1650 (3-C=O and amide C=O). ^1H NMR ($CDCl_3$) δ: 0.96 (t, 3H, CH_3CH_2, J=7.5 Hz), 2.03-2.09 (m, 2H, CH_3CH_2), 2.67 (s, 3H, $CH_{3\text{-pyridine}}$), 2.80 (s, 3H, $CH_{3\text{-pyridine}}$), 3.17-3.26 (m, 4H, 2x$CH_{2\text{-piperazine}}$), 3.79-3.96 (m, 4H, 2x$CH_{2\text{-piperazine}}$), 5.67 (t, 1H, CH_2CH(Br)CO, J=7.5 Hz), 6.93-7.27 (m, 6H, $H_{\beta\text{-pyridine}}$ + 5ArH). *Anal. Calcd*: C, 64.36; H, 6.38; N, 13.65. *Found*: C, 64.43; H, 6.59; N, 13.48.

4.1.4. Method for synthesis of 2-[(4,6-dimethylisothiazolo[5,4-*b*]pyridin-3-yl)oxy]propanoic acid (14) (Scheme 1)

4.1.4.1. Ethyl 2-[(4,6-dimethylisothiazolo[5,4-*b*]pyridin-3-yl)oxy]propanoate (7a) and its 2-N-substituted isomer (6a)

The mixture of 4,6-dimethylisothiazolo[5,4-*b*]pyridin-3(2*H*)-one **1** (5 mmol), potassium carbonate (5.5 mmol) and ethyl 2-bromopropanoate (5.5 mmol) in 30 mL of acetonitrile was heated to reflux and stirred for 3 h. The hot reaction mixture was filtered and evaporated to dryness. The residue was chromatograhed (CC; ethyl acetate/cyclohexane/chloroform 3:2:1) to give fractions containing 3-O-substituted isomer **7a** (Rf=0.79) and 2-N-substituted isomer **6a** (Rf=0.65, not described).

Anal. $C_{13}H_{16}N_2O_3S$ (m.w. 280.35); 45% yield, m.p. 38-39˚C. ^{1}H NMR ($CDCl_3$) δ: 1.26 (t, 3H, OCH_2CH_3, J=7.2Hz), 1.68 (d, 3H, $CH(CH_3)CO$, J=6.9), 2.64 (s, 3H, $CH_{3\text{-pyridine}}$), 2.73 (s, 3H, $CH_{3\text{-pyridine}}$), 4.19-4.26 (m, 2H, OCH_2CH_3), 5.46 (q, 1H, $CH(CH_3)CO$, J=7.2Hz), 6.96 (s, 1H, $H_{\beta\text{-pyridine}}$). *Anal. Calcd*: C, 55.70; H, 5.75; N, 9.99. Found: C, 55.32; H, 5.70; N, 8.99.

4.1.4.2. 2-[(4,6-dimethylisothiazolo[5,4-*b*]pyridin-3-yl)oxy]propanoic acid (14)

Compound **7a** (1 mmol) was dispersed in 30 mL of concentrated HCl (37%) and refluxed for 1 h. The mixture was cooled, filtered and the precipitate was dissolved in 30 mL of aqueous sodium bicarbonate (5%). The solution was filtered and acidified with hydrochloric acid (2N). The precipitate was filtered, washed with water, dried and crystallized from ethanol-water.

Anal. $C_{11}H_{12}N_2O_3S$ (m.w. 252,29); 87% yield, m.p. 178-180˚C. FT-IR (UATR, selected lines) ν_{max}/cm^{-1}: 3000-2500 br(OH), 1710 (C=O acid). ^{1}H NMR (DMSO-d_6) δ: 1.58 (d, 3H, $CH(CH_3)CO$, J=6.9), 2.57 (s, 3H, $CH_{3\text{-pyridine}}$), 2.66 (s, 3H, $CH_{3\text{-pyridine}}$), 5.31 (q, 1H, $CH(CH_3)CO$, J=6.9Hz), 7.20 (s, 1H, $H_{\beta\text{-pyridine}}$). *Anal. Calcd*: C, 52.37; H, 4.79; N, 11.10. *Found:* 52.48; H, 4.59; N, 10.72

4.1.5. General method for preparation of 2-[4-oxo-4-substituted-butyl]-4,6-dimethylisothiazolo[5,4-*b*]pyridin-3(2*H*)-one and 3-[4-oxo-4-substituted-butoxy]-4,6-dimethylisothiazolo[5,4-*b*]pyridine derivatives (17-20) (Scheme 1)

4.1.5.1. 4-(4,6-dimethyl-3-oxo-2,3-dihydroisothiazolo[5,4-*b*]pyridin-2-yl)butanoic acid (15) and 4-[(4,6-dimethylisothiazolo[5,4-*b*]pyridin-3-yl)oxy]butanoic acid (16)

Compounds **15** and **16** were prepared by acid-catalyzed hydrolysis of ethyl 4-(4,6-dimethyl-3-oxo-2,3-dihydroisothiazolo[5,4-*b*]pyridin-2-yl)butanoate **6b** or its 3-O-substituted isomer **7b** according to the procedure described in **4.1.4.1.**. The product was crystallized from ethanol-water.

4.1.5.1.1. 4-(4,6-dimethyl-3-oxo-2,3-dihydroisothiazolo[5,4-*b*]pyridin-2-yl)butanoic acid (15)

Anal. $C_{12}H_{14}N_2O_3S$ (m.w. 266.32); 87% yield, m.p. 141-143˚C. FT-IR (UATR, selected lines) ν_{max}/cm^{-1}: 3100-2400 br(OH), 1720 (C=O acid), 1650 (3-C=O). ^1H NMR (DMSO-d_6) δ: 1.83-1.87 (m, 2H, $CH_2CH_2CH_2$), 2.26 (t, 2H, CH_2CO, J=7.2), 2.53 (s, 3H, $CH_{3\text{-pyridine}}$), 2.63 (s, 3H, $CH_{3\text{-pyridine}}$), 3.81 (t, 2H, $N_{isothiazole}\text{-}CH_2$, J=6.9 Hz), 7.18 (s, 1H, $H_{\beta\text{-pyridine}}$). ^{13}C NMR (DMSO-d_6) δ: 17.70 (CH_3), 24.57 (CH_3), 30.72 (CH_2), 41.72 (CH_2), 45.28 (CH_2), 114.55 ($C_{\text{-pyridine}}$), 123.09 ($C_{\text{-pyridine}}$), 127.44 ($C_{\text{-pyridine}}$), 137.35 ($C_{\text{-pyridine}}$), 142.26 ($C_{\text{-pyridine}}$), 164.76 (CO), 176.42 (COOH). *Anal. Calcd*: C, 54.12; H, 5.30; N, 10.52. *Found:* C, 54.44; H, 5.47; N, 10.74.

4.1.5.1.2. 4-[(4,6-dimethylisothiazolo[5,4-*b*]pyridin-3-yl)oxy]butanoic acid (16)

Anal. $C_{12}H_{14}N_2O_3S$ (m.w. 266.32); 90% yield, m.p. 193-195˚C. FT-IR (UATR, selected lines) ν_{max}/cm^{-1}: 3200-2500 br(OH), 1710 (C=O acid). ^1H NMR (DMSO-d_6) δ: 2.01-2.05 (m, 2H, $CH_2CH_2CH_2$), 2.42 (t, 2H, CH_2CO, J=7.2), 2.56 (s, 3H, $CH_{3\text{-pyridine}}$), 2.62 (s, 3H, $CH_{3\text{-pyridine}}$), 4.46 (t, 2H, $N_{isothiazole}\text{-}CH_2$, J=6.3 Hz), 7.17 (s, 1H, $H_{\beta\text{-pyridine}}$). *Anal. Calcd*: C, 54.12; H, 5.31; N, 10.52. *Found:* C, 54.42; H, 5.26; N, 10.47.

4.1.5.2. 2-[4-oxo-4-substituted-butyl]-4,6-dimethylisothiazolo[5,4-*b*]pyridin-3(2*H*)-one and 3-[4-oxo-4-substituted-butoxy]-4,6-dimethylisothiazolo[5,4-*b*]pyridine derivatives (17-20)

1 mmol of 4-(4,6-dimethyl-3-oxo-2,3-dihydroisothiazolo[5,4-*b*]pyridin-2-yl)butanoic acid **15** or its 3-O-substituted isomer **16** in 30 mL of dichloromethane at 0°C (ice-bath) was treated with triethylamine (0.05 mL) and 1 mmol of ethyl chloroformate. After stirring the reaction mixture at 0°C for 15 min, 1.1 mmol of an appropriate amine derivative [1-(3-chlorophenyl)piperazine to obtain **17** and **18**, 1-phenylpiperazine to obtain **19** and **20**] was added to this solution. The final mixture was stirred at 0-25°C for 20 h. After this time the mixture was evaporated to dryness. The residue was chromatograhed and crystallized from appropriate solvents.

4.1.4.2.1. 2-{4-oxo-4-[4-(3-chlorophenyl)piperazin-1-yl]butyl}-4,6-dimethylisothiazolo[5,4-*b*]pyridin-3(2*H*)-one (17)

Anal. $C_{22}H_{25}ClN_4O_2S$ (m.w. 444.99); CC (ethyl acetate, R_f=0.25), 36% yield, m.p. 92-94˚C (ethanol). FT-IR (UATR, selected lines) ν_{max}/cm^{-1}: 1640 (3-C=O and amide C=O). ^1H NMR ($CDCl_3$) δ: 2.11-2.15 (m, 2H, $CH_2CH_2CH_2$), 2.43 (t, 2H, CH_2CO, J=7.2), 2.58 (s, 3H, $CH_{3\text{-pyridine}}$), 2.71 (s, 3H, $CH_{3\text{-pyridine}}$), 3.12-3.15 (m, 4H, $2xCH_{2\text{-piperazine}}$), 3.56 (t, 2H, $CH_{2\text{-piperazine}}$, J=6.9 Hz), 3.75 (t, 2H, $CH_{2\text{-piperazine}}$, J=6.9 Hz), 3.95 (t, 2H, $N_{isothiazole}\text{-}CH_2$, J=6.6 Hz), 6.75-7.19 (m, 5H, $H_{\beta\text{-pyridine}}$ + 4ArH). *Anal. Calcd*: C, 59.38; H, 5.66; N, 12.59. *Found:* : C, 59.62; H, 5.86; N, 12.66

4.1.4.2.2. 3-{4-oxo-4-[4-(3-chlorophenyl)piperazin-1-yl]butoxy}-4,6-dimethylisothiazolo[5,4-*b*]pyridine (18)

Anal. $C_{22}H_{25}ClN_4O_2S$ (m.w. 444.99); CC (ethyl acetate, R_f=0.54), 29% yield, m.p. 118-120˚C (ethanol). FT-IR (UATR, selected lines) ν_{max}/cm^{-1}: 1630 (amide C=O). ^1H NMR ($CDCl_3$) δ: 2.23-2.27 (m, 2H, $CH_2CH_2CH_2$), 2.57 (t, 2H, CH_2CO, *J*=7.2), 2.63 (s, 3H, $CH_{3\text{-pyridine}}$), 2.66 (s, 3H, $CH_{3\text{-pyridine}}$), 3.14-3.17 (m, 4H, 2x$CH_{2\text{-piperazine}}$), 3.61 (t, 2H, $CH_{2\text{-piperazine}}$, *J*=5.1 Hz), 3.77 (t, 2H, $CH_{2\text{-piperazine}}$, *J*=5.1 Hz), 4.58 (t, 2H, $N_{isothiazole\text{-}}CH_2$, *J*=6.3 Hz), 6.75-7.20 (m, 5H, $H_{\beta\text{-pyridine}}$ + 4ArH). *Anal. Calcd*: C, 59.38; H, 5.66; N, 12.59. *Found:* C, 59.72; H, 5.86; N, 12.59.

4.1.4.2.3. 2-[4-oxo-4-(4-phenylpiperazin-1-yl)butyl]-4,6-dimethylisothiazolo[5,4-*b*]pyridin-3(2*H*)-one (19)

Anal. $C_{22}H_{26}N_4O_2S$ (m.w. 410.54); CC (ethyl acetate, R_f=0.26), 32% yield, m.p. 81-83˚C (ethanol). FT-IR (UATR, selected lines) ν_{max}/cm^{-1}: 1640 (3-C=O and amide C=O). ^1H NMR ($CDCl_3$) δ: 2.12-2.17 (m, 2H, $CH_2CH_2CH_2$), 2.45 (t, 2H, CH_2CO, *J*=7.2), 2.60 (s, 3H, $CH_{3\text{-pyridine}}$), 2.72 (s, 3H, $CH_{3\text{-pyridine}}$), 3.17-3.21 (m, 4H, 2x$CH_{2\text{-piperazine}}$), 3.63 (t, 2H, $CH_{2\text{-piperazine}}$, *J*=6.6 Hz), 3.82 (t, 2H, $CH_{2\text{-piperazine}}$, *J*=6.6 Hz), 3.97 (t, 2H, $N_{isothiazole\text{-}}CH_2$, *J*=6.6 Hz), 6.94-7.30 (m, 6H, $H_{\beta\text{-pyridine}}$ + 5ArH). *Anal. Calcd*: C, 64.36; H, 6.38; N, 13.65. *Found:* C, 64.31; H, 6.57; N, 13.51.

4.1.4.2.4. 3-[4-oxo-4-(4-phenylpiperazin-1-yl)butoxy]-4,6-dimethylisothiazolo[5,4-*b*]pyridine (20)

Anal. $C_{22}H_{26}N_4O_2S$ (m.w. 410.54); CC (ethyl acetate/cyclohexane 2:2, R_f=0.23), 44% yield, m.p. 98-100˚C (ethanol). FT-IR (UATR, selected lines) ν_{max}/cm^{-1}: 1670 (3-C=O), 1630 (amide C=O). ^1H NMR ($CDCl_3$) δ: 2.24-2.28 (m, 2H, $CH_2CH_2CH_2$), 2.58 (t, 2H, CH_2CO, *J*=7.2), 2.64 (s, 3H, $CH_{3\text{-pyridine}}$), 2.67 (s, 3H, $CH_{3\text{-pyridine}}$), 3.15-3.19 (m, 4H, 2x$CH_{2\text{-piperazine}}$), 3.66 (t, 2H, $CH_{2\text{-piperazine}}$, *J*=4.8 Hz), 3.82 (t, 2H, $CH_{2\text{-piperazine}}$, *J*=4.8 Hz), 4.59 (t, 2H, $N_{isothiazole\text{-}}CH_2$, *J*=6.3 Hz), 6.94-7.32 (m, 6H, $H_{\beta\text{-pyridine}}$ + 5ArH). ^{13}C NMR ($CDCl_3$) δ: 19.06 (CH_3), 24.34 (CH_3), 29.67 (CH_2), 41.36 ($C_{\text{-piperazine}}$), 41.46 ($C_{\text{-piperazine}}$), 45.01 (CH_2), 49.78 ($C_{\text{-piperazine}}$), 49.89 ($C_{\text{-piperazine}}$), 67.66 (CH_2), 116.30 ($C_{\text{-pyridine}}$), 117.02 ($C_{\text{-pyridine}}$), 121.48 ($C\text{-}_{Ar}$), 129.37 ($C\text{-}_{Ar}$), 145.88 ($C_{\text{-pyridine}}$), 160.53 ($C_{\text{-pyridine}}$), 161.85 ($C_{\text{-pyridine}}$), 170.48 (CO), 176.56 (CO). *Anal. Calcd*: C, 64.36; H, 6.39; N, 13.65. *Found:* C, 64.03; H, 6.44; N, 13.35.

4.2 *In vitro* cyclooxygenase inhibitory activity

COX Colorimetric Inhibitor Screening Assay Kit (*Cayman Chemical Company, Ann Arbor, MI*)

This method allows one to estimate the peroxidase activity of COX by colorimetric monitoring of occurrence of the oxidized form of *N,N,N',N'*-tetramethyl-*p*-phenylenediamine (TMPD) at 590 nm. TMPD is a substrate for most enzymes with peroxidase activity, and high throughput microplate assays using TMPD allow the rapid screening of a wide range of therapeutics that inhibit COX activity *in vitro*.

The test is based on the oxidation of TMPD during the reduction of PGG_2 (prostaglandin G2) to PGH_2, which is reflected by a change in color, measured spectrophotometrically (Victor2 microspectrophotometer, PerkinElmer Waltham, MA, USA). The assay uses Tris-HCl buffer (0.1 M assay buffer, pH 8.0), a solution of heme in dimethylsulfoxide (DMSO), enzymes (COX-1, COX-2), arachidonic acid (100 µM), KOH (0.1 M) and a solution of TMPD. The assay mixture contains: 150 µL of assay buffer, 10 µL of heme, and 10 µL of COX-1 or COX-2. To the wells for determination of 100% enzyme activity (each COX sample was assayed in triplicate) were added 10 µL of the substances used as solvents (methanol, ethanol, DMSO). To the other wells were added 10 µL of tested inhibitors at appropriate concentrations. To all wells were added 20 µL of TMPD. The reaction was initiated by the addition of arachidonic acid.

The effect of tested inhibitors on COX-1 and COX-2 enzyme activity was measured by assaying the rate of TMPD oxidation within 2 minutes in a spectrophotometer at 590 nm.

We determined the activity factor at 2 min of incubation with the tested compounds in comparison to the initial activity of the enzyme. This enabled the calculation of IC_{50} values (concentrations at which 50% inhibition of enzyme activity occurred).

Statistical analysis

Statistical significance of the results was calculated with the paired *t*-test and with Two-way analysis of variance ANOVA, following the routine statistical methods.

4.3 Molecular docking

To date, in the Protein Data Bank (PDB) there are deposited 67 x-ray crystal structures of cyclooxygenases (COX), 27 of cyclooxygenase-1 (COX-1) and 40 of cyclooxygenase-2 (COX-2). Most of them were co-crystallized with ligands. In the absence of human enzymes the high-resolution and complete x-ray structures of murine cyclooxygenase crystallized for Cox-1 (PDB ID: 4O1Z) and Cox-2 (PDB ID: 4M11) variants co-crystallized with the same

ligand (meloxicam) were chosen for molecular docking. The sequence identity of the structures with human variants is very high (~95%) and the residues comprising the active sites are fully conserved, as described elsewhere.[17] In the preparation step, the protein models were verified in terms of chemical structure and the type of bonds. All cofactors were removed. To unify coordinates the structures were aligned using a multiple structural alignment algorithm (MUSTANG) implemented in Yasara 11.6.16.33. The program constructs a multiple alignment using the spatial information of the α-carbon atoms of the protein in the set. The ligands were built de novo in Spartan'10. The energies were minimized by the Hartree−Fock ab initio algorithm with the 6-31G* basis set. The compounds were exported as mol2 files and docked into the crystal structure. The docking study was performed in Molegro Virtual Docker 6.0, which was successfully applied by other investigators.[21-23] Comparisons of docking positions with crystal structure are in the supporting materials (Figure S3, Table S2). If not marked, the default settings were applied; the calculations were parameterized as follows: blind docking to whole binding domain, MolDock Score [GRID] searching and scoring algorithm, grid resolution 0.3 A., search area: x: 63.25 y: 23.03 z: 206.04, radius 15, number of runs: 1000, number of iterations: 1500, max population size 50, max number of poses return: 10.

Acknowledgements

The study was supported in part by the PL-Grid (Polish High Performance Computing Infrastructure). The authors greatly appreciate Prof. Krzysztof Jozwiak, Medical University of Lublin, Poland for access to the appropriate software.

References

1. Kirkby, N.S.; Chan, M.V.; Zaiss, A.K.; Garcia-Vaz, E.; Jiao, J.; Berglund, L.M.; Verdu, E.F.; Ahmetaj-Shala, B.; Wallace, J.L.; Herschman, H.R.; Gomez, M.F.; Mitchell, J.A. *Proc. Natl. Acad. Sci. U.S.A.* **2016**, *113*, 434.

2. Chandrasekharan, N.V.; Dai, H.; Roos, K.L.; Evanson, N.K.; Tomsik, J.; Elton T.S.; Simmons, D.L. *Proc. Natl. Acad. Sci. U.S.A.* **2002**, *99*, 13926.

3. Nandakishore, R.; Yalavarthi, P.R.; Kiran, Y.R.; Rajapranathi, M. *Curr. Drug Discov. Technol.* **2014**, *11*, 127.

4. Warner, T.D.; Giulliano, F.; Vojnovic, I.; Bukasa, A.; Mitchell, J.A.; Vane, J.R. *Proc. Natl. Acad. Sci. U.S.A* **1999**, *96*, 7563.

5. Unlu, S.; Onkol, T.; Dundar, Y.; Okcelik, B.; Kupeli, E.; Yesilada, E.; Noyanalpan, N.; Sahin, M.F. *Arch. Pharm.* **2003**, *336*, 353.

6. Banoglu, E.; Okcelik, B.; Kupeli, E.; Unlu, S.; Yesilada, E.; Amat, M.; Caturia, J.F.; Sahin, M.F. *Arch. Pharm.* **2003**, *336*, 251.

7. Gulcan, H.O.; Kupeli, E.; Unlu, S.; Yesilada, E.; Sahin, M.F. *Arch. Pharm.* **2003**, *336*, 477.

8. Raghavendra, N.M.; Jyothsna, A.; Rao, A.V.; Subrahmanyam, C.V.S. *Bioorg. Med. Chem. Lett.* **2012**, *22*, 820.

9. Eleftheriou, P.; Geronikaki, A.; Hadjipavlou-Litina, D.; Vicini, P.; Filz, O.; Filimonov, D.; Poroikov, V.; Chaudhaery, S.S.; Roy, K.K.; Saxena, A.K. *Eur. J. Med. Chem.* **2014**, *62*, 197.

10. Keri, R.S.; Patil, M.R.; Patil, S.A.; Budagumpi, S. *Eur. J. Med. Chem.* **2015**, *89*, 207.

11. Malinka, W.; Sieklucka-Dziuba, M.; Rajtar, G.; Zgodzinski, W.; Kleinrok, Z. *Pharmazie* **2000**, *55*, 416.

12. Malinka, W.; Swiatek, P.; Filipek, B.; Sapa, J.; Jezierska, A.; Koll, A. *Farmaco* **2005**, *60*, 961.

13. Zawisza, T.; Malinka, W. *Farmaco* **1985**, *40*, 124.

14. Malinka, W.; Ryng, S.; Sieklucka-Dziuba, M.; Rajtar, G.; Gowniak, A.; Kleinrok, Z. *Farmaco* **1998**, *53*, 504.

15. Krzyzak, E.; Sliwinska, M.; Malinka, W. *J. Fluoresc.* **2015**, *25*, 277.

16. Picot, D.; Loll, P.J.; Garavito, R.M. *Nature*, **1994**, *367*, 243.

17. Xu, S.; Hermanson, D.J.; Banerjee, S.; Ghebreselasie, K.; Clayton, G.M.; Garavito, R.M.; Marnett, L.J. *J. Biol. Chem.* **2014**, *289*, 6799.

18. Gierse, J.K.; McDonald, J.J.; Hauser, S.D.; Rangwala, S.H.; Koboldt, C.M.; Seibert, K. *J. Biol. Chem.* **1996**, *271*, 15810.

19. Dhanjal, J.K.; Sreenidhi, A.K.; Bafna, K.; Katiyar, S.P.; Goyal, S.; Grover, A.; Sundar, D. In PLoS One; **2015**; Vol. 10(8), e0134691, doi 10.1371, published online.

20. Blobaum, A.L.; Xu, S.; Rowlinson, S.W.; Duggan, K.C.; Banerjee, S.; Kudalkar, S.N.; Birmingham, W.R.; Ghebreselasie, K.; Marnett, L.J. *J. Biol. Chem.* **2015**, *290*, 12793.

21. Gogoi, D.; Bezbaruah, R.L.; Bordoloi, M.; Sarmah, R.; Bora, T.C. *Bioinformation* **2012**, *8*, 812.

22. Palkar, M.B.; Singhai, A.S.; Ronad, P.M.; Vishwanathswamy, A.H.; Boreddy, T.S.; Veerapur, V.P.; Shaikh, M.S.; Rane, R.A.; Karpoormath, R. *Bioorg. Med. Chem.* **2014**, *22*, 2855.

23. Urniaz, R.D.; Jozwiak, K. *J. Chem. Inf. Model.* **2013**, *53*, 1406.

24. Rowlinson, S.W.; Kiefer, J.R.; Prusakiewicz, J.J.; Pawlitz, J.L.; Kozak, K.R.; Kalgutkar, A.S.; Stallings, W.C.; Kurumbail, R.G.; Marnett, L.J. *J. Biol. Chem.* **2003**, *278*, 45763.